23/525

UCRL-JC-125444
PREPRINT

Experimental Investigation of the Compressible Richtmyer-Meshkov Instability from a Broad-Spectrum, Multimode Initial Perturbation

D. Farley, T. Peyser, P. Miller, L. Logory, P. Stry, E. Burke
Lawrence Livermore National Laboratory
Livermore, California 94550

This paper was prepared for submittal to the
6th International Workshop on Physics of Compressible Turbulent Mixing
Marseille, France
June 18-21, 1997

June 1997

Lawrence Livermore National Laboratory

Experimental Investigation of the Compressible Richtmyer- Meshkov Instability from a Broad-Spectrum, Multimode Initial Perturbation

D. Farley, T. Peyser, P. Miller, L. Logory, P. Stry, E. Burke
Lawrence Livermore National Laboratory
P. O. Box 808, L-22, Livermore, California, 94551, USA

Abstract: Experiments have been conducted using the Nova laser system to investigate the growth of the Richtmyer-Meshkov (RM) instability resuling from a strong shock wave (M$\sim$ 30) crossing a prescribed well-defined initial multimode perturbation. The perturbation was a 100 mode superposition of 1 μm amplitude sine waves with randomly generated phases between 0 and 2π. The two working fluids were fluidized brominated plastic and carbon resorcinol foam, giving a post-shock Atwood number of approximately 0.6. The present experimental results give a power-law coefficient of 0.87 $\pm$ 0.2 for the growth of the interface. This value is higher than results previously published.

1. Introduction

The Rayleigh-Taylor (RT) and Richtmyer-Meshkov (RM) hydrodynamic instabilities can occur across an interface between fluids of differing densities. The Rayleigh-Taylor instability occurs whenever a lower density fluid is supporting the lighter fluid against an imposed acceleration, whereas the Richtmyer-Meshkov instability occurs when a shock wave crosses the density interface from either direction. Simple analytical solutions are available for the linear growth of the RT and RM instabilities [*e.g.*, Taylor (1950), Richtmyer (1960), Meshkov (1969), Brouillette & Sturtevant (1993), Haan (1989), and Alon et al. (1995)]. Some experimental and numerical results are also available for single-mode and multimode initial perturbations [*e.g.*, Remington et al. (1994), Grove (1993), Youngs (1994), Peyser et al. (1995), and Dimonte et al. (1997)]. However, further effort is needed in describing the non-linear growth of these instabilities. In particular, further quantitative analysis of the growth of multimode perturbations into the non-linear regime is required. In the present research, the growth of the compressible RM instability resulting from an initial, well-defined multimode perturbation is analyzed utilizing experimental results from the Nova laser system. As has been previously published [Alon et al. (1995)], the growth of bubble and spike fronts are predicted to follow a power-law time dependence, as given by

$$\delta \sim t^{\theta} \tag{1}$$

where δ is the distance of the bubble or spike penetration into the other fluid,t is time, and θ is the power-law coefficient. According to analytical and computational results of Alon et al Alon et al. (1995), θ should equal approximately 0.4 for bubbles. It is believed that this value is insensitive to Atwood number [$A=(\rho_2 - \rho_1)/(\rho_2 + \rho_1)$]. For spikes, θ should vary from approximately 1 for A = 1 to 0.4 for low Atwood numbers. No analysis is made as to Mach number effects. In the present experiments, the growth of the mix region for a well-defined multimode perturbation will be analyzed to obtain θ for A = .6 at a high Mach number (M$\sim$ 30).

†For more information - Email: dfarley@llnl.gov

2. Experimental

Experiments were done using the Nova laser system. With Nova, up to ten beams can be directed to experimental packages within a vacuum chamber to conduct high energy density experiments. In the present experiments, eight beams are used to drive a strong shock wave into a miniature shock tube while two beams are used as backlighter sources. The eight drive beams are directed into opposite ends of a gold Hohlraum which has a shock tube mounted as shown in Fig. 1. The Hohlraum is a 3 mm long and 1.5 mm diameter hollow cylinder. Typically, a 1 ns square pulse of approximately 20 kJ of 0.35 μm wavelength light strikes the interior of the Hohlraum whereupon the laser energy is absorbed by the gold and emitted as x-rays. A quasi-Planckian temperature profile with a characteristic temperature of approximately 230 eV is generated within the Hohlraum which is then utilized as a source for the initiation of the ablation and shock fronts into the the target material. The initial strength of the resulting shock wave is about 85 Mbar, which decays to 35 Mbar near the density interface, and has a Mach number of approximately 30. The design of the shock tube and target were such that a

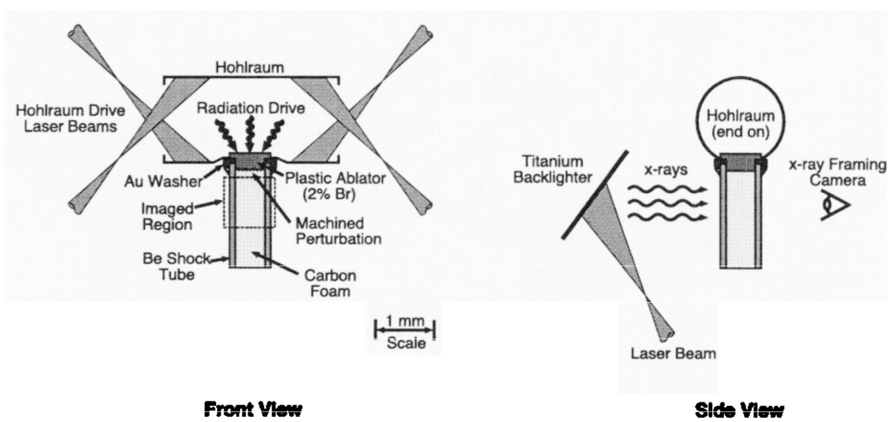

Figure 1. Experimental package mounted to a gold Hohlraum

strong, planar shock wave would travel from heavy fluid to light and that the growth of the mix region could be seen at both early and late times. The shock tube itself is made of beryllium with an outer diameter of 700 μm and inner diameter of 500 μm and an overall length of 2200 μm. The payload within the shock tube consists of a high density ablator and low density foam. The heavy ablator material (1.22 g/cc) is made of polystyrene doped with 2% bromine. The bromine serves a dual purpose both as a means to increase the opacity of the plastic for imaging contrast as well as to absorb the incident x-ray energy. A tophat structure is utilized on the end of the ablator at the attachment to the Hohlraum, as shown in Fig. 1. The tophat has an outer diameter of 700 μm and a thickness of 100 μm which extends into the Hohlraum cavity. This tophat design was found to aid in shock planarity [Peyser et al. (1995)]. The two-dimensional multimode perturbation is machined into the end of the ablator at the density interface. The multimode perturbation is rectilinear, and is a superposition of 100 sine waves (100 modes), each wave having a.1 μm amplitude and a randomly generated phase between 0 and 2π. The wavelength of each mode varied linearly from 10 μm to 100 μm in 0.90 μm increments. The profile of the machined surface and its corresponding power spectrum is shown in Fig. 2. Shown adjacent to the ablator in Fig. 1 is a low density carbon resorcinol foam (0.1 g/cc). This results in a pre-shock Atwood number of 0.85. The foam is much less opaque to x-rays than the ablator material which aids in visualizing the growth of the interface. As the shock wave crosses the perturbed interface, the interface subsequently inverts, and the shock then continues into the foam payload. The resulting post-shock Atwood number is approximately 0.6. The growth of the interface can then be recorded using x-ray imaging.

Backlighting of the shock tube was achieved by focusing two of the Nova beams onto a titanium foil mounted approximately 4 mm from the shock tube, normal to the camera line of sight and on the opposite side of the shock tube from the imaging camera. The titanium foil is 3-4 mm on a side and 25 μm thick, and emits 4.7 keV x-rays upon illumination by the Nova beams. These x-rays then propagate through the shock tube and are differentially attenuated depending on the relative opacity of the working fluids. An x-ray framing camera is then used to record the images. These cameras are described elsewhere [Remington et al. (1992), Budil et al. (1996)]. Images are typically recorded at times between 5 to 15 ns.

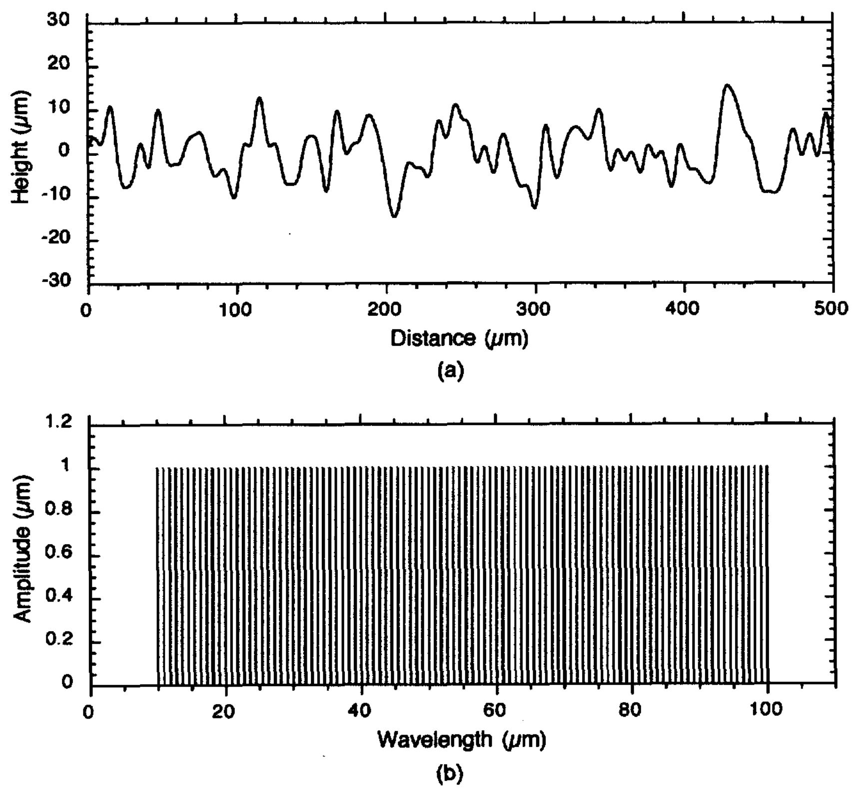

Figure 2. (a) Multimode rectilinear surface which was precision machined into the brominated plastic ablator, and (b) power spectrum of the perturbation modes

3. Results

Typical images of the experiment recorded by the x-ray framing camera are shown in Fig. 3. These images are taken at 13, 14, and 15 ns. The shock crosses the perturbation at approximately 4 ns. It can be seen from the progression of frames in Fig. 3 that there is growth of relatively large structures within the mixing region. The shocked foam behind the shock can also be seen. Bubbles penetrate into the brominated plastic ablator, but because of the higher opacity of the ablator material, it is difficult to directly observe bubble structure in this region. To quantify the width of the mixing region, a 100 μm wide vertical lineout is extracted from the x-ray framing camera images. Within this lineout is contained the unshocked foam region, the shock discontinuity, the shocked foam, the mix region, and the opaque ablator

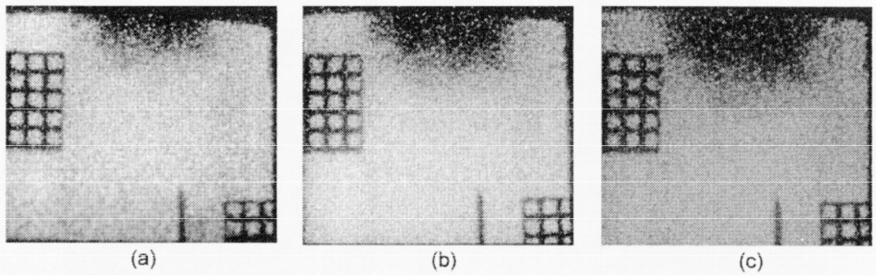

Figure 3. Framed x-ray images of the experiment depicting the opaque ablator region, the mix region, the compressed foam region and the unshocked foam at (a) 13 ns, (b) 14 ns, (c) 15 ns

region. Because the backlighter intensity profile is typically Gaussian in shape, the transmitted intensity distribution recorded by the x-ray framing camera includes this Gaussian profile. A least-squares Gaussian shape is fitted to the vertical lineout, and this fit is then divided out of the lineout. A typical normalized lineout is shown in Fig. 4. Identified in Fig. 4 is the foam region, the shock, the shocked foam region, the mix region, and the shocked brominated plastic region. A 5-95 % transmission criteria across the mix region of the lineout is then used to obtain a quantitative mix width. Mix widths were obtained as outlined above at

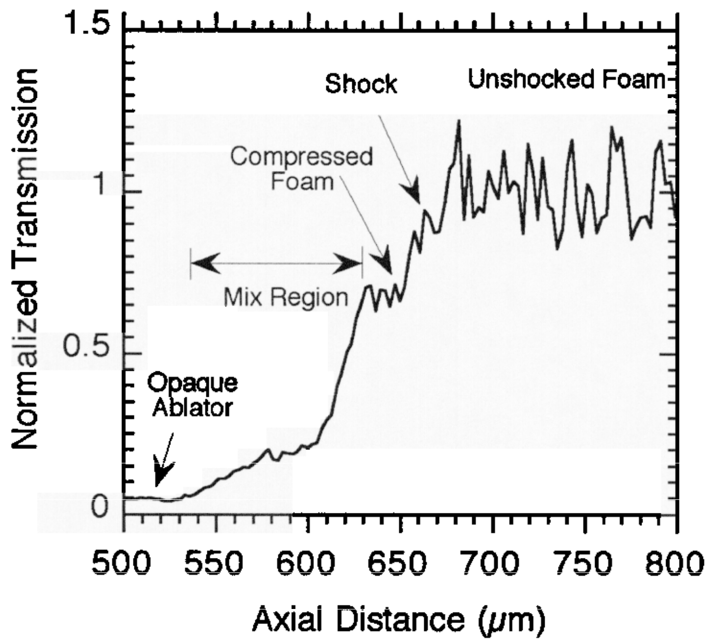

Figure 4. Normalized 100 μm wide vertical lineout of x-ray transmission through the opaque ablator region, the mix region, the compressed foam region and the unshocked foam region

times between 5 and 15 ns using many Nova laser shots. To compare with theoretical models, however, the effect of decompression should be removed from the mix width data. The fluids experience decompression in these experiments due to the blow-off of ablated plastic in addition to the reflected expansion wave which is generated when the shock is incident upon the density interface. Theoretical models generally do not account for such decompression effects. The two-dimensional arbitrary-Lagrange-Eulerian code called CALE was used to simulate this type of experiment. Through the use of tracers within computational simulations of the experiment using CALE, the expected decompression of the target was calculated. Experiments fielded on

Nova confirmed decompression calculations [Peyser et al. (1995)]. This data was used to correct the experimental mix width data for decompression effects. The decompression-corrected mix width data is plotted in Fig. 5. Error bars were obtained by averaging multiple data points occurring at similar times and using their corresponding standard deviations.

To obtain the power-law coefficient θ from this data, log scales were used in plotting the data set shown in Fig. 5. This logarithmic data is shown in Fig. 5 along with a least- squares linear fit with the late-time data occurring between 8 ns and 15 ns. Before 8 ns it is believed that all the modes have not yet reached a fully non-linear state, and therefore the linear fit is done for times later than 7 ns. From this linear fit, a power-law coefficient θ of 0.87 ± 0.2 is obtained for the two-dimensional rectilinear 100-mode initial perturbation. It should be noted, however, that this coefficient is obtained from mix width data which includes both the bubble and spike regions. However, as numerical CALE simulations have shown, at the high Mach numbers found in these experiments ($M \sim 30$) bubble and spike structure and growth are nearly symmetric. With this assumption, the power-law coefficient presently obtained should be valid for both the bubble and spike fronts. The present coefficient value of 0.87 is higher than 0.4 predicted

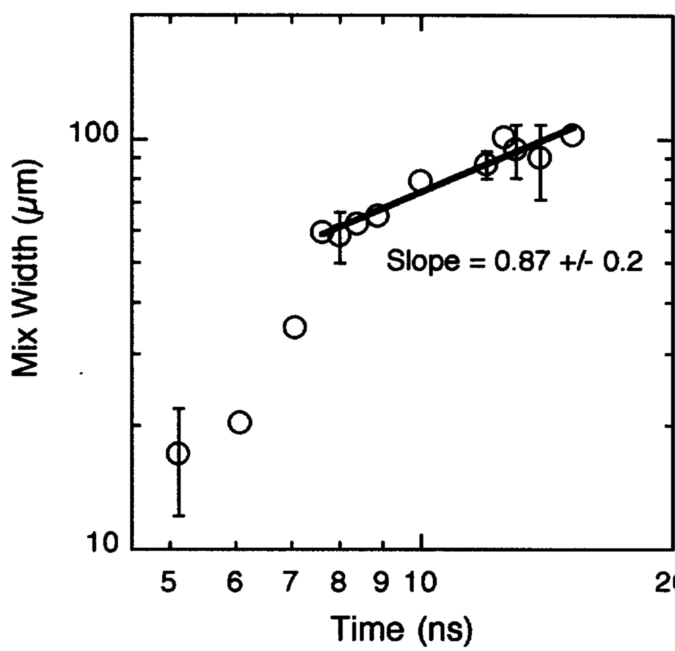

Figure 5. Experimental mix width results showing a power-law time dependence of 0.87 resulting from a strong shock crossing an initial perturbation of100 modes

by Alon et al. [Alon et al. (1995)] for bubble growth, and also higher than 0.5 published by Dimonte et al. [Dimonte et al. (1997)]. In the work of Alon et al [Alon et al. (1995)], bubble and spike fronts were considered separately with each material having a different value for θ, depending on the Atwood number of the flow. They also were considering low Mach number flows where the spikes and bubbles do not necessarily grow symmetrically. In Dimonte's work, three-dimensional perturbations were used, which may result in different mode coupling effects from the present 2-D experiments. Three-dimensional perturbations were achieved in Dimonte's experiments through sandblasting or electric discharge machining of the interface. Although this process may roughen the surface, it was only possible to estimate the average wavelength of the perturbations. The considerable experimental difficulty associated with characterizing three-dimensional targets precluded quantitative knowledge of the actual surface profile. In the present experiments, the specified rectilinear 100 mode perturbation was precision machined into the ablator interface and was closely examined for each target manufactured. Differences in the experimental configuration, target type, drive energy and pulse shape, and also in the analysis procedure may be responsible for the discrepencies from the present experiments.

An examination of published data suggests that high amplitude, long wavelength modes present at the interface may dominate the evolution of the instability. From the beginning of the development of the present experiments, a well-defined mode structure of the initial condition of the perturbation was determined to be essential for the mix results to be valuable. The reason for this is that multimode perturbations could refer to a variety of different perturbation types. In the present experiments, only the phase of each mode is random, while the amplitudes and wavelengths of the modes are specified. It is possible, in fact probable, that differing modal structures of multimode perturbations may produce different power-law coefficients. Therefore, it is important to quantify such modal structures, and to conduct experiments with differing modal structure variants in order to investigate the nature of the evolution of the multimode Richtmyer-Meshkov instability.

4. Conclusion

Experiments have been conducted using the Nova laser system to investigate the growth of the Richtmyer-Meshkov (RM) instability resulting from a strong shock wave ($M \sim 30$) crossing a prescribed well-defined initial multimode perturbation. The perturbation was a 100 mode superposition of 1 μm amplitude sine waves with randomly generated phases between 0 and 2π. The experimental package was a reduced-scale shock tube mounted to a 3 mm long gold Hohlraum used in Nova experiments. The two working fluids were fluidized brominated plastic (CH + 2% Br) and carbon resorcinol foam, giving a post-shock Atwood number of approximately 0.6. The growth of the mixing region is expected to follow a power-law behavior with time. The present experimental results give a power-law coefficient of 0.87 ± 0.2. This value is higher than results previously published. The discrepency with other results may be due to 2-D versus 3-D effects, or differing experimental conditions.

Further experiments are being conducted to investigate the effect differing modal structure shapes on RM growth. From initial results, it is believed that qualitatively and quantitatively different structural growth of the mixing region can be expected from these different multimode perturbations.

Acknowledgement. The authors would like to thank the individuals who support these experiments (including taget development, fabrication and assembly, and technical support) and the Nova operations personnel.

This work was performed under the auspices of the U.S. Department of Energy by Lawrence Livermore National Laboratory under Contract No. W-7405-Eng-48.

References

Alon U, Hecht J, Ofer D and Shvarts D, Phys. Rev. Lett., 74, 534 (1995).
Brouillette M and Sturtevant B, Phys. Fluids, 5, 4, 916, (1993).
Budil KS, et al, Rev. Sci. Instrum., 67, 485 (1996).
Dimonte G, Phys. Plasmas, (currently under review,1997).

Grove JW, et al, Phys. Rev. Lett., 71, 3473 (1993).
Haan SW, Phys. Rev. A, 39, 5812 (1989).
Meshkov E, Sov. Fluid Dyn., 4, 101 (1969).
Peyser TA, et al, Phys. Rev. Lett., 75, 2332 (1995).
Remington BA, et al Rev. Sci. Instrum., 63, 5083 (1992).
Remington BA, et al, Phys. Rev. Lett., 73, 545 (1994).
Richtmyer RD, Commun. Pure Appl. Math., XIII, 297 (1960).
Taylor G, Proc. R. Soc. London, Ser. A, 201, 192 (1950).
Youngs DL, Laser Particle Beams, 12 (1994).

Technical Information Department • **Lawrence Livermore National Laboratory**
University of California • Livermore, California 94551